Ocean Engineering 159 (2018) 410–421

Contents lists available at ScienceDirect

Ocean Engineering

journal homepage: www.elsevier.com/locate/oceaneng

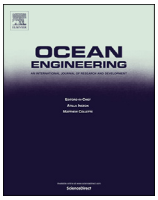

Flow behavior behind a clockwise-and-counterclockwise rotational oscillating cylinder

Yangyang Gao [a,*], Kang Yang [a], Xingyue Ren [b,**], Baofeng Zhang [c], Soon Keat Tan [d]

[a] Ocean College, Zhejiang University, Zhoushan, 316021, PR China
[b] College of Civil Engineering and Architecture, Hainan University, Haikou, 570228, PR China
[c] Powerchina Huadong Engineering Corporation Limited, Hangzhou, 311122, PR China
[d] Maritime Research Centre, School of Civil and Environmental Engineering, Nanyang Technological University, 639798, Singapore

ARTICLE INFO

Keywords:
Flow behavior
Clockwise-and-counterclockwise rotation
PIV
Rotational angular amplitude

ABSTRACT

Flow characteristics downstream of a rotational oscillating cylinder at Reynolds number Re = 300 was investigated. The experiments were conducted using a model cylinder in a recirculating open water channel and the flow field was captured by using the Particle Image Velocimetry (PIV) technique. The model cylinder was set to undergo clockwise-and-counterclockwise rotation at selected angular amplitude (angular amplitude α varying from 0° to 360°) and at the lock-on frequency ratio $F_r = 1.0$ (where $F_r = f_n/f_v$, the ratio of the forcing frequency f_n to the natural vortex shedding frequency f_v). The effects of rotational movement of the cylinder on the near wake downstream of the cylinder were interpreted in terms of the instantaneous vorticity patterns, as well as the time-averaged streamline topology, mean velocity distributions and Reynolds shear stress contours. Based on the observation of the flow patterns and vortex contours, it was deduced that the clockwise-and-counterclockwise rotation produced significant effect on the wake and modified the wake flow structures and vortex shedding patterns. The time-averaged streamline structures appeared to be non-symmetrical about the longitudinal axis of the flow.

1. Introduction

The phenomenon of flow-induced vibration of circular cylinder has drawn considerable interest over the past decades as the phenomenon has been identified as the cause of fatigue damage in offshore structures, such as risers, mooring lines and in power plants such as heat exchangers. Understandably, the flow-induced vibration is at its strongest when the vortex shedding frequency in the wake is the same as the forcing frequency of the cylinder, namely the lock-on phenomenon. It is the consensus that such vibration is most undesirable. To date, most of the reported investigations on flow-induced vibration have been mainly concentrated on a cylinder undergoing inline and transverse oscillations with respect to the flow direction (Williamson and Roshko, 1988; Khalak and Williamson, 1996; Sarpkaya, 2004; Gabbai and Benaroya, 2005; Chaplin et al., 2005; Williamson and Govardhaan, 2008). Impact of forced rotation on the wake of a rigidly mounted cylinder (for example, drilling-riser) has not been investigated as widely. Some of the recent experimental and numerical works can be found in Filler et al. (1991); Mahfouz and Badr (2000); Mittal and Kumar (2003); Bourgue and Jacono (2014) and Sellappan and Pottebaum (2014).

Most of the reported experimental studies for the rotationally oscillating cylinder were focused on the flow behaviors based on the flow visualization technique. Tokumaru and Dimotakis (1991) conducted an experimental study on flow past an oscillating cylinder at Reynolds number Re = 15000 (Re $= U_0D/\upsilon$, where D was the cylinder diameter, U_0 was the free-stream velocity and υ was the kinematic viscosity) using flow visualization and laser-Doppler velocity measurements. The forcing dimensionless velocity amplitudes varied from 0 to 16 and forcing Strouhal number from 0.17 to 3.3. Four distinct flow modes at different forcing condition and significant reduction of VIV at high forcing frequency were observed. Based on the findings obtained using hot-wire anemometry and smoke-wire flow visualization, Fujisawa et al. (2001) proposed a method for actively controlling vortex shedding behind a circular cylinder at Re = 6700 and 20000 through rotational oscillations. They found that the velocity fluctuations and the fluid forces were reduced by the feedback control with the optimum values of phase lag

---

* Corresponding author.
** Corresponding author.
E-mail addresses: yygao@zju.edu.cn (Y. Gao), oceanxyr@163.com (X. Ren).

https://doi.org/10.1016/j.oceaneng.2018.04.053
Received 21 August 2017; Received in revised form 1 April 2018; Accepted 16 April 2018

and feedback gain. Thiria et al. (2006) found that the structure of the shed vortex and fluctuations of drag coefficients were strongly affected by the forcing parameters, such as the forcing amplitude and the ratio of forced and natural frequencies of the vortex shedding. They also found that the forced wake is characterized by a "lock-on" region where the vortices were shed at the forcing frequency and a region where the vortices could be reorganized to produce a second frequency close to that for the "unforced" wake. Lee and Lee (2006) found that the lock-on phenomenon always occurred at $F_r = 1.0$ (F_r defined as the ratio of the forcing frequency f_n to the natural vortex shedding frequency f_v) and the frequency range of lock-on regime expanded with increasing oscillation amplitude. They also found that the drag coefficient was reduced when F_r was less than 1.0 at a constant oscillation amplitude of 30°. Lee and Lee (2008) further found that, depending on F_r, three well-defined flow regimes could be discerned: i.e. non-lock-on, transitional and lock-on regimes. Nazarinia et al. (2012) investigated flow past a cylinder subjected to combined translational and rotational oscillations and found that both V_r (the ratio between the translational and rotational velocities) and F_r had significant effects on the synchronization of the near-wake vortex structures. Kumar et al. (2013) observed that rotary oscillations of a cylinder had significant effect on the wake structure. The lock-on of the wake to the forcing frequency depended not only on the forcing parameters but also on the downstream distance from the cylinder.

To the authors' knowledge, the experimental investigations on flow past a rotational oscillating cylinder were mostly performed at high Reynolds numbers $\mathrm{Re} \geq 2000$ or low Reynolds number $\mathrm{Re} \leq 185$ (Gao et al., 2017). Due to the limitation of the experimental conditions, few experimental investigations were performed at $\mathrm{Re} = 300$ or in the vicinity of $\mathrm{Re} = 300$. For example, Taneda (1978) investigated the effect of the control parameters on the two-dimensional wake flow behind a rotational oscillating cylinder for $30 \leq \mathrm{Re} \leq 300$. In the further study of Wu et al. (1989), the control parameters was found to be strongly affected the fluid forces acting on the cylinder at $\mathrm{Re} = 300$. However, very little is known about the flow characteristics behind the cylinder undergoing a clockwise-and-counterclockwise rotation at $\mathrm{Re} = 300$. Moreover, the effect of rotational angular amplitude on the flow pattern remains to be elucidated. Therefore, the purpose of the present study was to investigate the flow behavior behind a clockwise-and-counterclockwise rotational oscillating cylinder at a lock-on frequency ratio of $F_r = 1.0$ for $\mathrm{Re} = 300$. The forcing rotational angular amplitude α was varied from 0° to 360°. The flow field behind the rotational oscillating cylinder was captured by using the Particle Image Velocimetry (PIV) technique. The effects of forcing rotational angular amplitude on the near wake were deduced based on the patterns of instantaneous vorticity, as well as the time-averaged streamline topology, mean velocity distribution and Reynolds shear stress contours.

2. Experimental setup

The experiments were performed in a recirculating open water channel, 6 m long and a rectangular cross-section of $0.3m \times 0.4m (W \times H)$, at the Maritime Research Center, Nanyang Technological University. Details of the water channel can be found in Gao et al. (2013). The model used in this experiment was a brass cylinder of diameter $D = 30$ mm, with a length of $L = 500$ mm. The blockage ratio D/W of the test cylinder was about 10%, smaller than the blockage ratios adopted in the experimental study of Fujisawa et al. (2001), Lim and Lee (2003) and Braza et al. (2006), which were about 20%, 25% and 20.8%, respectively. The effect of blockage ratio was considered to be ignored in the present study. The water depth was 300 mm, the clearance between the cylinder and the water channel bottom was about 3 mm (0.1D), resulting into an aspect ratio of 9.9 (≈10), similar to Wang et al. (2013), where the clearance between the cylinder and the water channel bottom was about 2 mm ($0.1D$). The effect due to vortex interaction along the span of the cylinder on the shedding behavior at the mid-plane was likely to be minimal (Norberg, 2003; Lau et al., 2004). The aspect ratio was considered to be large enough to ensure the two-dimensional flow at the mid-plane (Slaouti and Gerrard, 1981; West and Apelt, 1993; Lam and Zou, 2009; Wang et al., 2013; Ma et al., 2018). Fig. 1 shows a definition sketch of the experimental setup. As shown in Fig. 1, the laser sheet was positioned for the measurements in the horizontal (x-y) plane at the mid-height of water depth $H_s = 150$ mm, the camera was placed under the test section, perpendicular to the horizontal plane, which means that the field of view was taken from the bottom of water channel.

The cylinder was forced to rotate in a clockwise-and-counterclockwise manner about its longitudinal axis and with different angular amplitude α ranging from 0° to 360° and at 30° increments using a stepper motor. The rotational speed and angular amplitudes were precisely controlled by a programmable controller. The pre-set rotational frequency was set to equal to the natural vortex shedding frequency behind the stationary cylinder, that is the frequency ratio $F_r = 1.0$. The freestream velocity was about 0.01 m/s, and the corresponding Reynolds number $\mathrm{Re} = U_0 D/\upsilon$ was 300. In order to ensure the uniformity of the inlet flow, the stilling chamber upstream of the contraction fitted with perforated steel plates and a honeycomb screen was adopted (Gao et al., 2010, 2013). The uncertainty in this study was estimated, using a 95% confidence interval, to be less than 2.5% for the freestream velocity U_0, and the free-stream turbulence intensity in the test section was estimated to be less than 0.2%.

In this study, the PIV system (LaVision model) was used to capture the flow field behind the rotational oscillating cylinder. The particles were illuminated using light from a Quantel System double cavity Nd: YAG laser with a wavelength of 527 nm and a 2 mm thick laser sheet (power ~120 mJ per pulse, duration~5 ns). The flow is seeding using the neutrally buoyant hollow glass spheres (Spherocel® 110P8) with approximate diameter of 10–15 μm as the tracer particles, which offered good traceability and scattering efficiency. The particle images were recorded using a 12-bit charge-coupled device (CCD) camera, and had a resolution of $1.6K \times 1.2K$ pixels and a frame rate of 15 Hz. Based on a compromise between the requirements of recording a large field of view and resolving detailed flow structures, the viewing area was chosen to be about $130mm \times 180mm$. The LaVision Davis software was used to process the raw particle images and determine the flow fields. Velocity vectors were determined using the FFT (Fast-Fourier-Transform) method based on cross correlation algorithm with the standard Gaussian sub-pixel fit structured as an iterative multi-grid method. The processing procedure included two passes, starting with a grid size of 64 × 64 pixels, stepping down to 32 × 32 pixels overlapping by 50%, which gives a spatial resolution of 7500 vectors in the viewing area. Then a 3 × 3 median filter was applied to remove possible outliers in the vector map. The central vector was then replaced with the averaged vector obtained from the neighboring interrogation windows if it had deviated by more than 5 times the RMS (root-mean-square) value of the eight surrounding neighbours. For the smoothing process, the 3 × 3 average filter was chosen to establish the final vector maps. For each case, a set of 1050 frames of the instantaneous flow fields was acquired (i.e. 70 s recordings).

3. Results and discussion

3.1. Instantaneous flow patterns

Flow past a rotational oscillating cylinder was examined over a range of rotational angular amplitudes α = 0°-360°, and special attention was paid on the instantaneous flow field during an oscillation period at a constant frequency ratio $f_n/f_v = 1.0$. Details of the findings are discussed in the following sections. The instantaneous vorticity contours $\omega^* = \omega_Z D/U_0$ behind the rotational oscillating cylinder at different rotational angular amplitudes are shown in Fig. 2, where the solid and dashed lines represent positive and negative values, respectively. The instantaneous vorticity fields clearly show that the rotational angular amplitude has significant effect on the wake flow structures. Different vortex shedding modes are observed for various rotational angular amplitudes α. For all of